Structure-function correlations of rat trigeminal primary neurons: Emphasis on club-like endings, a vibrissal mechanoreceptor

By Sotatsu TONOMURA,[*1] Satomi EBARA,[*1,†] Knarik BAGDASARIAN,[*2] Daisuke UTA,[*3,*4] Ehud AHISSAR,[*2] Inbal MEIR,[*2] Ilan LAMPL,[*2] Daichi KURODA,[*1] Takahiro FURUTA,[*5] Hidemasa FURUE[*3] and Kenzo KUMAMOTO[*1]

(Communicated by Kunihiko SUZUKI, M.J.A.)

Abstract: This study focuses on the structure and function of the primary sensory neurons that innervate vibrissal follicles in the rat. Both the peripheral and central terminations, as well as their firing properties were identified using intracellular labelling and recording in trigeminal ganglia *in vivo*. Fifty-one labelled neurons terminating peripherally, as club-like, Merkel, lanceolate, reticular or spiny endings were identified by their morphology. All neurons responded robustly to air puff stimulation applied to the vibrissal skin. Neurons with club-like endings responded with the highest firing rates; their peripheral processes rarely branched between the cell body and their terminal tips. The central branches of these neurons displayed abundant collaterals terminating within all trigeminal nuclei. Analyses of three-dimensional reconstructions reveal a palisade arrangement of club-like endings bound to the ringwulst by collagen fibers. Our morphological findings suggest that neurons with club-like endings sense mechanical aspects related to the movement of the ringwulst and convey this information to all trigeminal nuclei in the brainstem.

Keywords: primary sensory neuron, intracellular recording, vibrissa, mechanoreceptor, club-like ending, ringwulst

Introduction

More than a century ago, primary sensory neurons were characterized as pseudo-unipolar cells.[1)] A single axon leaves the cell body and divides into two processes, one traveling towards the periphery that terminates as sensory endings and another that extends centrally to terminate on postsynaptic neurons within cranial and spinal nerve nuclei. In this way, individual primary sensory neurons transmit information collected from within their receptive fields to nuclei within the central nervous system.

The facial skin of many mammals possesses a dense sensory innervation in the mystacial pad, which contains vibrissal follicles arranged in regular rows. Sensory nerves in the facial skin are innervated by neurons whose cell bodies are situated within the trigeminal ganglia. Vibrissal follicles differ from common hairs because of their larger size and possession of two blood-filled sinuses, one, an upper, open ring sinus and the other, a lower cavernous sinus covered with a thick collagen capsule. Vibrissal follicles have been shown to be associated with a dense distribution of several kinds of mechanoreceptors.[2)–6)] Together, the vibrissal follicle and its associated sinuses, have been designated as the follicle sinus complex (FSC).[2)] Vibrissal mechanoreceptors in the rat have been classified by their

[*1] Department of Anatomy, Meiji University of Integrative Medicine, Nantan, Kyoto, Japan.
[*2] Department of Neurobiology, Weizmann Institute of Science, Rehovot, Israel.
[*3] Department of Information Physiology, National Institute for Physiological Sciences, Okazaki, Aichi, Japan.
[*4] Department of Applied Pharmacology, Graduate School of Medicine and Pharmaceutical Sciences, University of Toyama, Toyama, Japan.
[*5] Department of Morphological Brain Science, Graduate School of Medicine, Kyoto University, Kyoto, Japan.
[†] Correspondence should be addressed: S. Ebara, Department of Anatomy, Meiji University of Integrative Medicine, Honoda, Hiyoshi-cho, Nantan 629-0392, Japan (e-mail: s_ebara@meiji-u.ac.jp).

Note: The first two authors contributed equally to this work.

Abbreviations: FSC: follicle-sinus complex; TG: trigeminal ganglion.

doi: 10.2183/pjab.91.560

morphological features into: Merkel, lanceolate, club-like and Ruffini-like endings.[6)]

Sensory pathways from the skin to the cortex have been studied extensively;[7)–15)] however, relatively little information has been adduced on the relationships between the different mechanoreceptors and the electrophysiological responses of their primary neurons. Our aim is to rectify this deficiency using intracellular labelling and recording *in vivo* to identify receptor types and characterize the physiological responses of the primary sensory neurons associated with them.

Recently, we successfully detected several kinds of mechanoreceptors in the skin innervated by trigeminal neurons (*cf.* Ref. 16). In this study, we focused on the morphological and physiological aspects only of a unique mechanoreceptor in vibrissal follicles, the club-like ending.[6)]

Materials and methods

Forty-nine male Wistar rats (3 to 13 weeks old, weighing 40 to 300 g), were used in this study. All procedures were approved by the Meiji University of Integrative Medicine Animal Care and Use Committee (# 22-16), consistent with NIH guidelines for animal care.

Surgery for accessing the trigeminal ganglion. Under deep anaesthesia (sodium pentobarbital, 40 mg/kg, i.p. and urethane 1.2–1.5 g/kg, i.p.), animals were fixed in a stereotaxic apparatus and presented continuously with a mixture of 95% O_2 and 5% CO_2 via their nostrils. Rectal temperature was maintained at 37–38 °C by means of a heating pad placed beneath them. A 5 mm square area of bone situated 4–7 mm and 1–2 mm distant from the sagittal and coronal sutures, respectively, was removed from the right side of the skull (Fig. 1a). Portions of the underlying cortex and white matter were suctioned out to view the surface of the trigeminal ganglion, without damaging the thalamus (Fig. 1b). A plastic tube was placed on the trigeminal ganglion and filled with 0.9% sodium chloride solution (NaCl) to avoid desiccation of the tissue.

Intracellular recordings and labelling. Dura mater overlying the trigeminal ganglion was cut to allow the insertion of a glass microelectrode (20–80 MΩ, TW150F-4 WPI, P-97 Sutter Instrument) filled with 20% neurobiotin (Vector Lab. Inc., Burlingame, CA USA) dissolved in 1.0 M potassium acetate. Intracellular recordings were taken from single trigeminal ganglion cells, using an amplifier (IR-183, Cygnus Technology, USA) and an A/D converter (Power Lab 8/30, AD Instruments, New Zealand) connected to a computer operated by a recording and analysing software (Chart 5, AD Instruments).

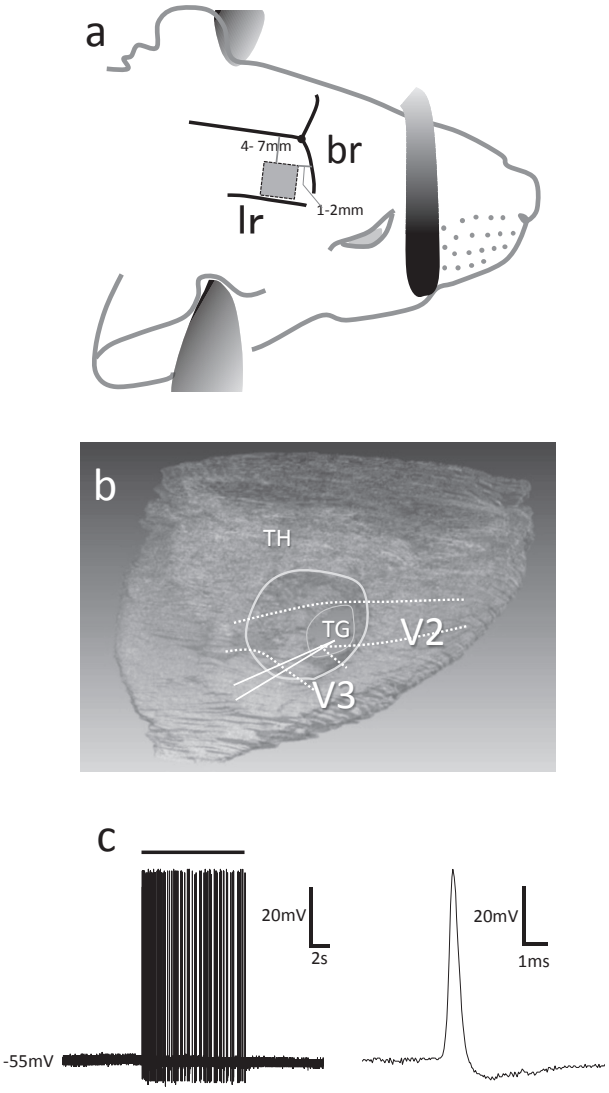

Fig. 1. a) Shaded square area of illustration of the temporal bone (5 mm^2) excised during our approach to the trigeminal ganglion. br; Bregma, lr; Lateral ridge of parietal bone. b) Three-dimensional reconstruction of the brain illustrating the location of the trigeminal ganglion (TG) with respect to the thalamus (TH), maxillary (V2) and mandibular (V3) nerves. Area circumscribed in white indicates the region of grey matter removed prior to recording from TG neurons. c) Representative trace of a TG neuron. A bunch of action potentials induced by stimulation (bar) of whiskers during recording from a TG neuron. Spontaneous firing was not observed. An enlargement of one action potential is shown at the right.

A resting membrane potential was detected following insertion of the glass microelectrode into

the ganglion cell. Then, action potentials elicited by mechanical stimulation applied to the skin of the face, including the mystacial pad, were recorded (Fig. 1c). Mechanical stimulation was applied by pushing the skin manually with a Von-Frey filament (ranging from 0.16 to 300 g), whisker bending by using a wooden-stick or Von-Frey filament (300 g) manually, and/or air puff stimulation (0.1–0.03 MPa, 10 s by a self-manufactured air puff stimulator). Neurons having a resting membrane potential more positive than −30 mV, or that were not able to maintain a stable membrane potential for more than 10 min, were excluded from the present analysis.

After recording the single cell intracellular responses to the mechanical stimulation, neurobiotin was electrophoretically injected into the ganglion cells via the recording electrode (0.2–0.5 nA, 750 ms, 1 Hz, 13–110 min); responses to mechanical stimulation were recorded again in order to identify any change in the post-injection responses. Finally, the cavity above the trigeminal ganglion was filled with medical cotton and covered with skin stuck together with medical grade glue.

Analysis of electrophysiology. Intracellular responses were recorded from all labelled ganglion cells prior to labelling the neurons by the intracellular injection of neurobiotin. The maximal values of the firing frequency (impulses per each second) were compared among the labeled neurons that responded to air-puff stimulation (0.1–0.03 MPa).

Visualization of labelled neurons. Following a survival time of 20 to 24 hours, deeply anaesthetized animals were perfused transcardially at room temperature with 50 ml of 0.9% NaCl followed by 100 to 150 ml of a fixative containing 4% paraformaldehyde buffered with 0.1 M sodium phosphate buffer (PB). Facial skin, the trigeminal nerve, trigeminal ganglion (TG), brain stem and spinal cord (∼C2 level) were removed and then immersed in 30% sucrose in 0.1 M PB prior to freeze cutting of serial sections (60–100 µm-thick) with a cryostat (Leica CM3050S). The trigeminal nerve bundles were placed into 0.1 M phosphate buffered saline (PBS) containing 0.1% Triton-X100 (PBS-T) and separated with forceps into tiny bundles.

All tissues were rinsed several times in PBS-T before, during, and after the procedures used to visualize neurobiotin using fluorescent conjugated streptavidin combined with a tyramide signal amplification (TSA) methods (*cf.* Ref. 17). Briefly, the tissues were immersed in a horseradish peroxidase conjugated avidin-biotin complex (ABC, 1 : 300, Vector Labs, USA) in PBST at room temperature for 3–6 hours, and were then reacted with TSA-biotin solution (1 : 90,000, RT, 1–3 hrs, PerkinElmer, USA). Prior to soaking in Alexafluor 594 conjugated streptavidin (1 : 500, Invitrogen, USA), the sections were again reacted with ABC, in order to visualize the labelled neurons. All tissues were mounted between two cover slips using Vectashield mounting medium (Vector Labs).

In order to relate the labelled axon to entire patterns of innervation in the skin, immunofluorohistochemistry was employed to visualize nerve fibers using primary antibodies to protein gene product 9.5 (rabbit anti-PGP9.5, 1 : 10,000, Ultraclone, England) for axons, S100 protein (mouse anti-S100b, 1 : 10,000, Invitrogen) for Schwann cells and myelin basic protein (rat anti-MBP, 1 : 500, Invitrogen) for myelin sheath with appropriate secondary antibodies labelled by Alexafluor 488 (1 : 500, Invitrogen) (for a detailed protocol, see Ref. 18).

Both serial sections and dissected bundles of nerve fibers were examined using a fluorescent microscope (E-800, Nikon, Tokyo, Japan) or confocal laser microscope (C1, Nikon). High resolution digital photomicrographs were obtained with a DXM1200 camera (Nikon) using NIS-Element DS (Nikon). Stacks of images were reconstructed in three dimensions and analysed using VGStudio Max 2.0 software (Volume Graphics Ltd., Heidelberg, Germany).

Instances in which more than one labelled neuron was detected in the ganglion were excluded from analysis; only neurons that were clearly labelled and their peripheral processes traced to their receptive fields were analysed.

Electron microscopy processing, observation and axonal tracing on serial semi-thin sections. Individual vibrissal follicles were dissected from the mystacial pad of the rats. These tissues were immersed immediately into 2% glutaraldehyde in 0.1 M PB for 3 hours followed by 1% osmic acid in 0.1 M PB for 2 hour at 4 °C followed by dehydration with an ascending series of acetone, and then embedded in Epon (Nakarai, Kyoto, Japan). Ultrathin sections were stained with uranyl acetate and lead citrate prior to examination with the electron microscope (JEM1220, JEOL, Tokyo, Japan).

A delta vibrissal follicle was cut into a longitudinal serial of 1 µm-thick sections and stained with toluidine blue. The serial sections were examined and digital photomicrographs made of all regions that included club-like endings. All serial images were

Table 1. Number of TG neurons whose mechanoreceptors well-labeled

Ending Type	area		total; 51 TG neurons		
			FSCs (40)		
vibrissal follicle sinus complex (FSC)	mystacial pads (34*)	eye lid (2), cheek (2)	air puff trial		total animals
			trials/animals	max amp	
Merkel endings at rete rigde collar	2	-	1/1	4	12
Merkel endings at level of ring sinus	8	1 (eye lid), 1 (cheek)	7/3		
lanceolate endings	7**	-	14/6	6	7**
club-like ***ringwulst*** **endings**	14	1 (eye lid), 1 (cheek)	13/8	8	16
reticular endings	4	-	7/3	3	4
other type of mechanoreceptors	1 (spiny ending)	-	-	-	1
not associated with FSCs	common hairs	touch domes	none FSCs (11)		
palisade endings innervating common hairs	8^{+}	-	8^{+}		
Merkel endings in hairy skin	-	3^{++}	3^{++}		

*; 36 FSCs in 34 mystacial pads. Three endings were recognized in a mystacial pad at the same time.
**; All but 1 circumferential ending were longitudinal.
+; mystacial pad (2), eye lid (1), upper lip (2), lower lip (1) and edge of mouth (2). ++; eye lid (1), upper lip (1) and cheek (1).

aligned and all club-like endings within the follicle, as well as their afferents, were marked individually using Adobe Photoshop (CS4) to make a stack image for three-dimensional analysis using VGStudio Max software.

Another vibrissal follicle was cut into 1 µm-thick serial sections and examined with a scanning electron microscope (TM3030, Hitachi High-Technologies Co., Tokyo, Japan). This approach was applied to regions at the level of the ring sinus without staining.

Results

Intracellular labelling. Intracellular recordings and neurobiotin injections were performed in the trigeminal ganglion of 49 anesthetized rats. A total of 62 cells responded to facial skin stimuli and were labelled with neurobiotin. Fifty-one of the 62 labelled cells were traced successfully to their terminals in the periphery, 12 of the 51 were also traced to their central terminations. The remaining 11 non-traceable neurons were excluded from this study. Three endings originating from different cell bodies were recognized in three separate FSCs in the same mystacial pad.

Labelled cell bodies and their axons in the trigeminal ganglion (TG) and the maxillary nerve were identified using three-dimensional analysis. Only the most intensively labelled axons were traced from cell bodies in the TG along their entire course to their peripheral terminations. In most instances, neurobiotin injections of 20–30 minute duration were sufficient to a clearly label of the entire course of the axons up to their peripheral terminals.

None of the 40 labelled peripheral branches that terminated in FSCs showed any ramification outside the capsule of a FSC. Moreover, no neuron innervated more than one FSC.

Of the 51 TG labelled neurons, 16 terminated as club-like endings, where 14 were located in FSCs of the whisker pad while the other 2 were in upper eyelid (1) and cheek skin (1) (Table 1, Fig. 2). The other 35 labelled mechanoreceptors included 24 cells whose peripheral axons terminated in vibrissal FSCs: 12 were Merkel, 7 lanceolate, 4 reticular and 1 spiny. The peripheral axon terminations of the remaining 11 cells, 8 palisade (lanceolate) and 3 Merkel endings, were not associated with a whisker FSC (Table 1). Each TG neuron possessed only a single type of mechanoreceptor at its termination.

Electrophysiological analysis of labelled neurons with club-like endings. Firing properties of all neurons projecting to the mechanoreceptors in the FSCs were analysed and a comparison between the different groups of mechanoreceptors was made (club-like ($N = 8$), Merkel ($N = 4$), lanceolate ($N = 6$), and reticular ($N = 3$) ending neurons). Air puff stimulation (0.1–0.03 MPa, 10 s) applied to all whiskers on the mystacial pad evoked a remarkably higher average maximal firing frequency of action potentials evoked in the neurons with club-like

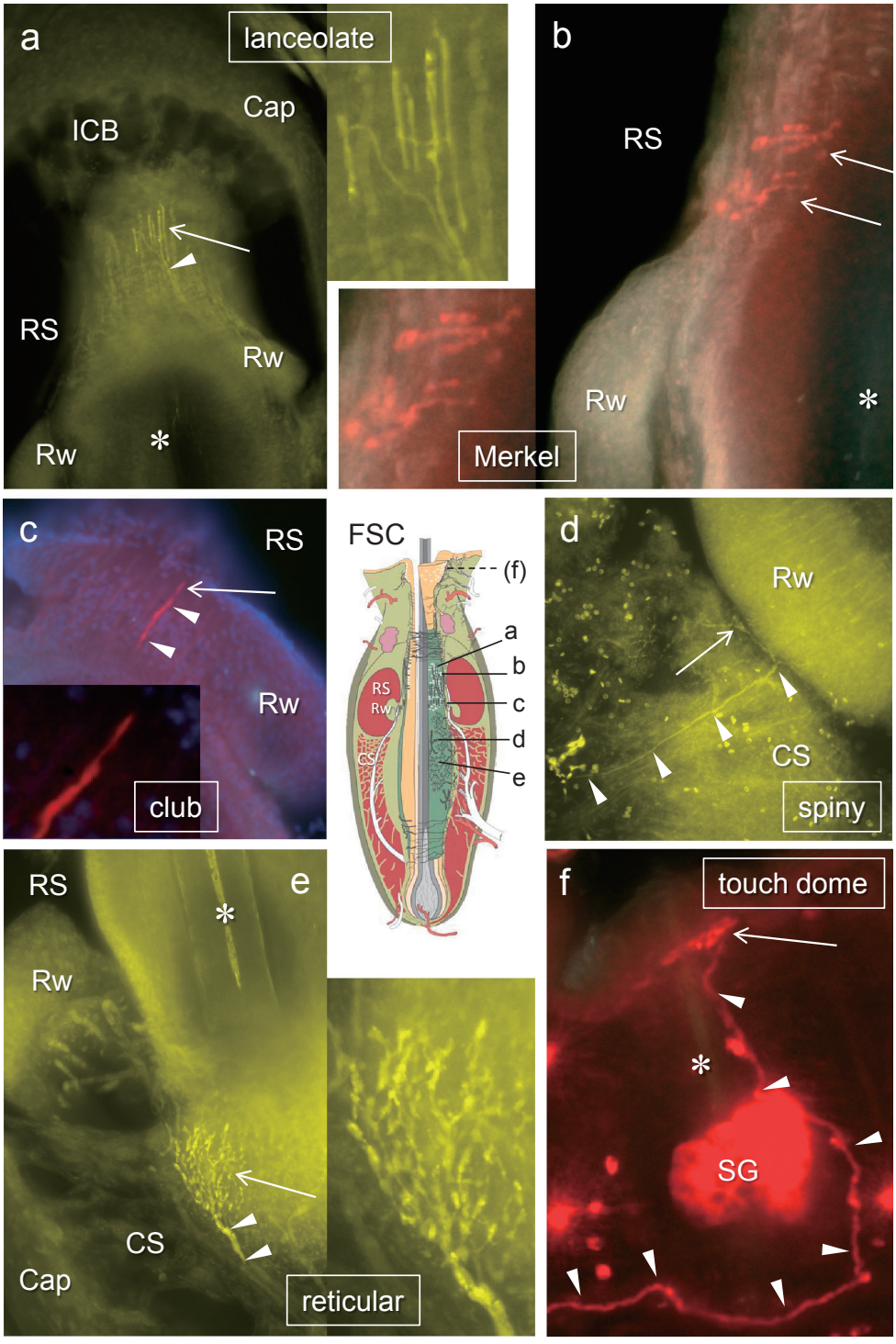

Fig. 2. All labelled neurons were recognized and differentiated according to their morphologies. a) Longitudinal lanceolate endings distributed at the level of the ring sinus (RS), b) Merkel endings at the level of the RS, c) club-like ending at the ringwulst (Rw), d) spiny endings at the level of the cavernous sinus (CS), e) reticular endings at the revel of the CS, f) Merkel endings at a touch dome on the eyelid. arrowheads; labelled axon, arrow; mechanoreceptor, asterisk; hair shaft, Cap; capsule of FSC, ICB; inner conical body, SG; sebaceous gland. A schematic drawing of vibrissal follicle-sinus complex (FSC), a modified image from our previous study (Ebara *et al.*, JCN, 2002),[6] indicates each position of those mechanoreceptors. Only f is out of FSC. Fig. a, d and e are pseudo-color images taken by a monochrome camera. b, c and f are real color images. Only c showed nuclei stained (purple) with DAPI.

endings (292.3 ± 95.6 Hz (mean $\pm$ SD)) than in all other mechanoreceptor neurons (135.1 ± 73.2 Hz, $P < 0.001$) namely; Merkel (92.6 ± 49.5 Hz, $P < 0.01$), lanceolate (183.4 ± 76.7 Hz, $P < 0.05$) and reticular (95.2 ± 28.3 Hz, $P < 0.01$) (Fig. 3, Table 1).

Full visualization of single trigeminal neurons. Each trigeminal neuron was fully visualized throughout its entire length from the cell body to the terminations of both the peripheral and central axon. One of the 16 neurons with club-like endings which was fully traced towards both the peripheral and central directions is shown in Figs. 4 and 5. The labelled stalk emerging from the cell body soon divided into two processes in opposite directions. The peripheral process never divided during its course to the club-like ending at the level of the ringwulst in the delta FSC. The central process of that neuron divided only in the trigeminal tract of the pons and gave collaterals. The parent axon gave rise to 23 collaterals that segmentally terminated mostly throughout the trigeminal nuclei of the brainstem in a stepwise fashion.

The course of the labelled neuron was reconstructed in all tissues except the maxillary nerve through which it passed in order to reconstruct three-dimensional structure (Figs. 4b, d). The image represented about 29 mm-long segment from the peripheral tip in the mystacial pad to the final termination around the uppermost level of the spinal cord. The basic structure of the pseudo-unipolar neurons was similar for all mechanoreceptor types although the peripheral branching patterns differed (Fig. 2).

In this study, we focused only on club-like endings (16 labelled neurons) because of their relatively simple and systematic distribution and morphology in the FSCs (Figs. 4, 5) with high capacity of neuronal responses to mechanical stimulation (Fig. 3). The firing frequencies of evoked action potentials in all other types of mechanoreceptor neurons were defined in order to compare them with club-like endings.

Peripheral processes of labelled neuron with club-like endings. Sixteen neurons terminated as club-like endings in the principal FSCs of β, γ, δ (2), B1, C1, C2, D2, D3, E1, E2, E5 and labial small FSCs (2), the rostral FSC on the eye lid, and the FSC on the cheek skin at each ringwulst respectively (Fig. 6). Eleven of the 16 peripheral processes having club-like endings did not branch between the cell body and the axon terminal (Figs. 4, 5). The remaining 5 peripheral processes each divided once into two myelinated nerve fibers inside the FSC. Their terminal branches gave rise to axon terminals in close proximity to each other, but the terminals were not adjacent.

Detailed structure of club-like endings in three-dimensional reconstruction analysis. All ringwulsts showed a sausage-like shape from a top view of the reconstructed mystacial pad (Fig. 6). They were situated at the lower region of the ring sinus (Figs. 6a, 7a). Their location at the hair shaft was approximately three fifths of the distance between the hair bulb to the skin surface. Each ringwulst pointed to a deficient part at the dorso-caudal position (Figs. 6, 7). The ringwulst was connected to the outer root sheath having a thin layer of mesenchymal sheath. The contacting surface was restricted only to the upper part of the ringwulst, so that it seemed as if the ringwulst were hanging from the mesenchymal sheath in the ring sinus (Fig. 7).

Morphological aspects of neurons with club-like endings associated with the ringwulst were studied both by light microscopy (as a series of 1 µm-thick sections), as well as by electron microscopy (Fig. 7). Club-like endings, 30 to 40 µm long, and 5 to 9 µm wide that terminated as only one unbranched receptor were related to myelinated afferents of Aβ or occasionally Aδ groups (Fig. 7).

The afferents of 48 of the 52 club-like endings were associated with axon terminals; the remaining 4 neurons demonstrated the convergence of two axon terminals arranged side-by-side into one afferent fiber. Nine of the 52 axon terminals ended in a ball-like swollen appendage (Fig. 7d).

All endings were arranged longitudinally at regular intervals within the level of the contacting surfaces between the ringwulst and the mesenchymal sheath. Few club-like ending were observed at the deficient part of the ringwulst (Figs. 7b, d). A large portion of all club-like endings was situated between the glassy membrane and the ringwulst. Each club-like ending was directly connected with dense collagen fibrils that projected to the ringwulst (Figs. 7g, h). However, direct contacts were not observed between the glassy membrane and the ending (Figs. 7f, i) at its opposite side.

Axon terminals contained mitochondria and numerous neurofilaments. They were surrounded by Schwann cell sheaths with containing many mitochondria, covered by a dense layer of collagen fibrils and an outer wrapping of one or two thin fibroblast layers (Figs. 7i, j).

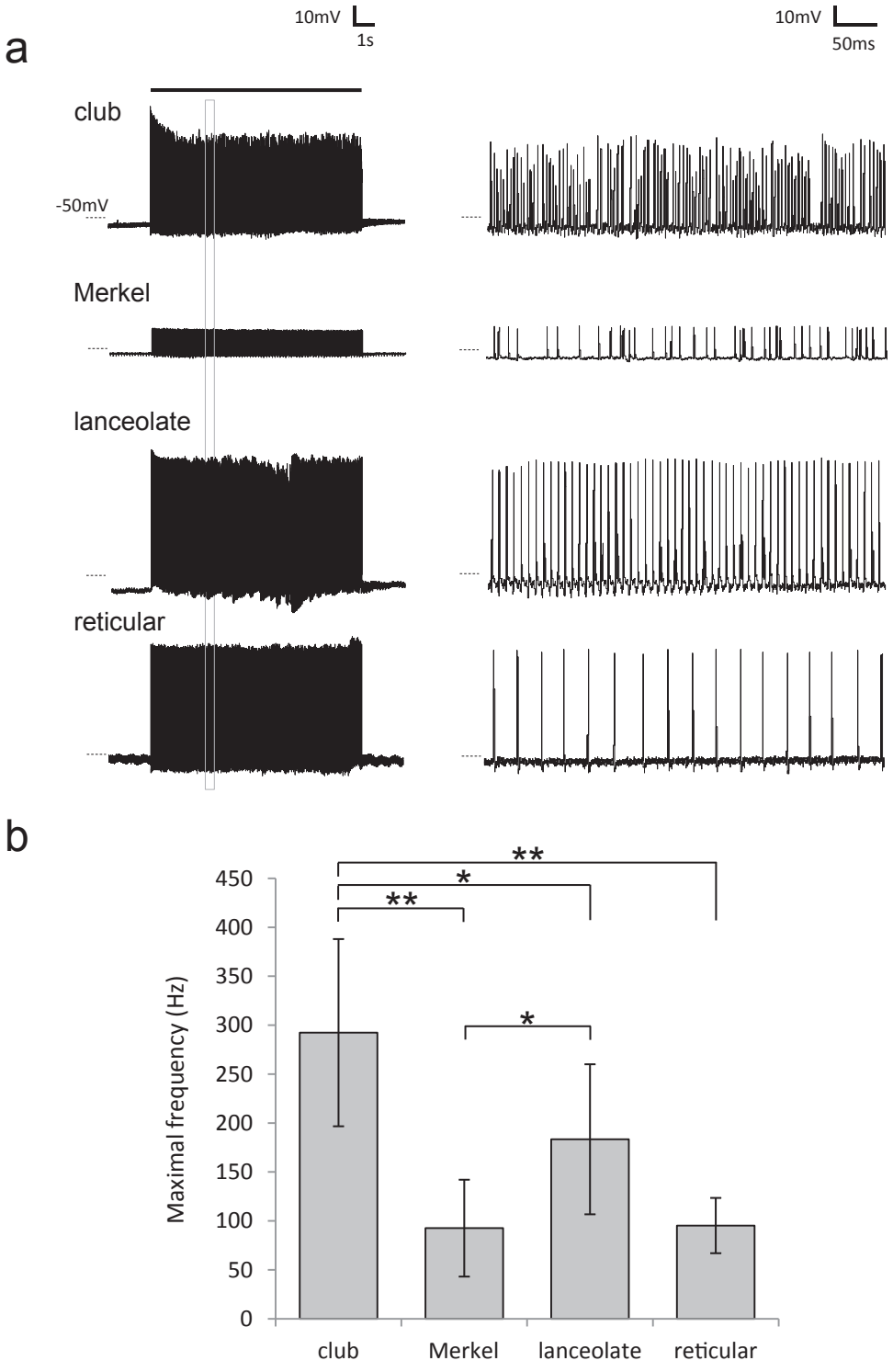

Fig. 3. a) Response potentials of labelled four neurons evoked by 10-second air puff stimulation (0.1–0.03 MPa). At the right, about 400 ms of the 3rd second (square) were enlarged for each tracing. b) The maximal frequency (mean ± SD) during every 1 second of the air puff stimulation in labelled neurons with club-like endings compared to other labelled mechanoreceptor neurons. *; $P < 0.05$, **; $P < 0.01$ (Student's *t*-test).

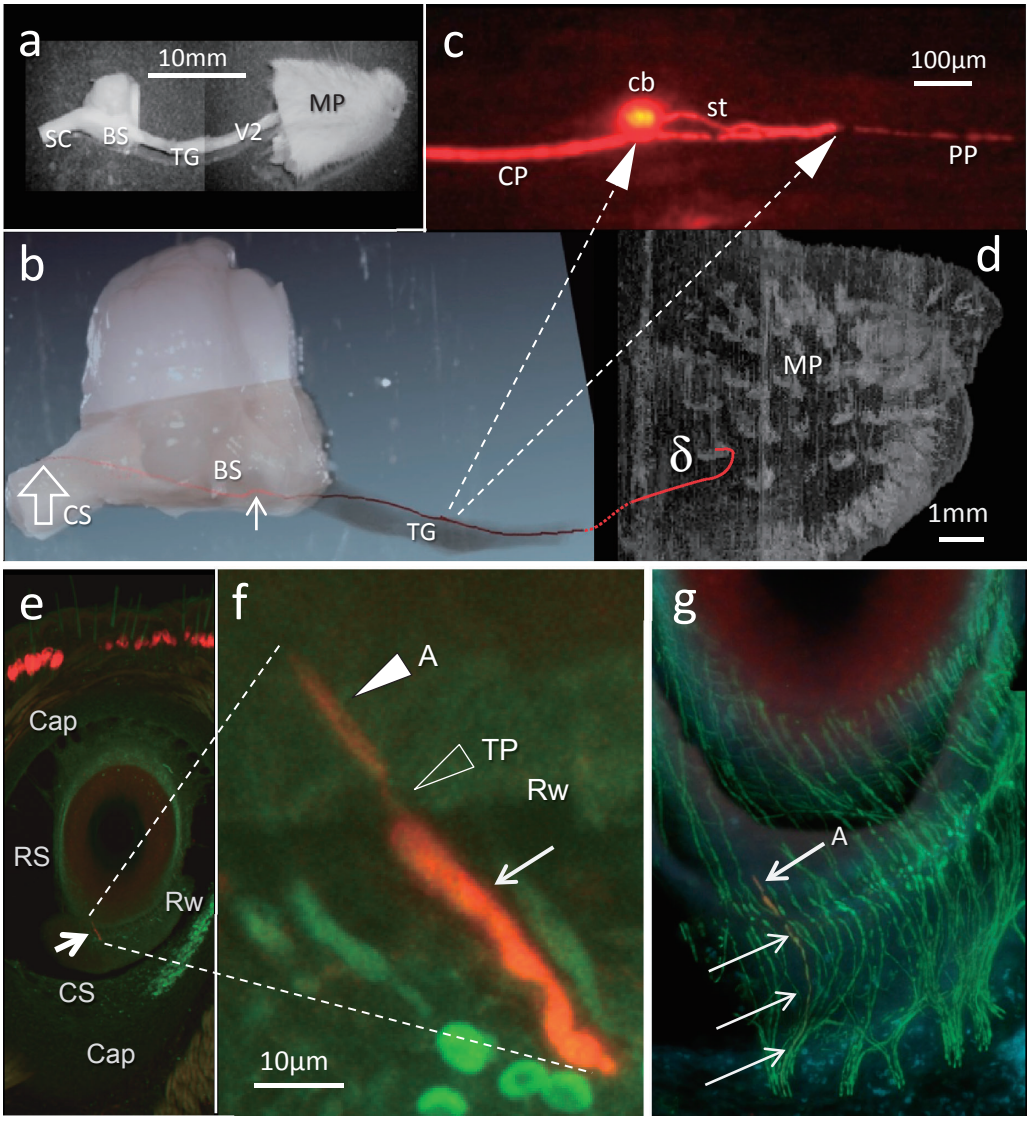

Fig. 4. a) Dissected tissue including Mystacial Pad (MP). BS; brainstem, SC; spinal cord, TG; trigeminal ganglion, V2; maxillary nerve. b) A visualized and reconstructed trigeminal ganglion (TG) neuron (red) combined with a higher magnification image of a. The first collateral emitted at a distance of approximately 5 mm from the ganglion cell body (small arrow). Open arrow; the end of the central branch of the neuron. c) A higher magnification of the TG neuron in b. Two arrows in dashed line; a round cell body (cb) and the branching point of the stalk (st) into the peripheral (PP) and central (CP) branches are indicated in relation with b. d) A reconstructed three-dimensional image of a mystacial pad evenly enlarged to b. Lower magnification photos of serial 100 µm-thick sections were used. Red line; the peripheral branch labelled neuron in b terminated the delta FSC. e) A microphotograph of a section of the delta FSC including the club-like ending (arrow) of the labelled neuron indicated in b. Cap; capsule, RS; ringsinus, Rw; ringwulst, CS; cavernous sinus. f) A higher magnification image of the club-like ending in e with guidance by two dashed lines. Arrow; a labelled axon, TP; terminal point (open arrowhead), a filled white arrowhead; axon terminal. g) A photomontage of confocal images of 4 serial sections indicating the labelled axon (arrows) and the club-like ending (A) in f (red). Non labelled axons were visualized in green by immunohistochemistry focused on PGP9.5, a pan axonal marker.

Fig. 5. a) Montage of three-dimensional reconstructions displayed at high magnification, confocal microscopic images of the central branch of the labelled neuron in Fig. 4. Origins of collateral branches are numbered 1 through 23 proceeding centrally. The first collateral from the ganglion cell body (small arrow). The 23rd collateral is recognized C1 level of the spinal cord (open thick arrow). The main branch in between 16 and 17 lacks any collaterals. Upper insertion is a part of the same image in 4b. The lower insertion is a horizontal top view of the three-dimensional reconstruction indicating the labelled axon in red. PrSV; trigeminal principal sensory nucleus, SpVO, SpVI, SpVC; trigeminal spinal nucleus oral part, interpolar part, caudal part respectively. b) Higher magnification view of a at the part of the 7th–16th collaterals. (*Continued on the following page*)

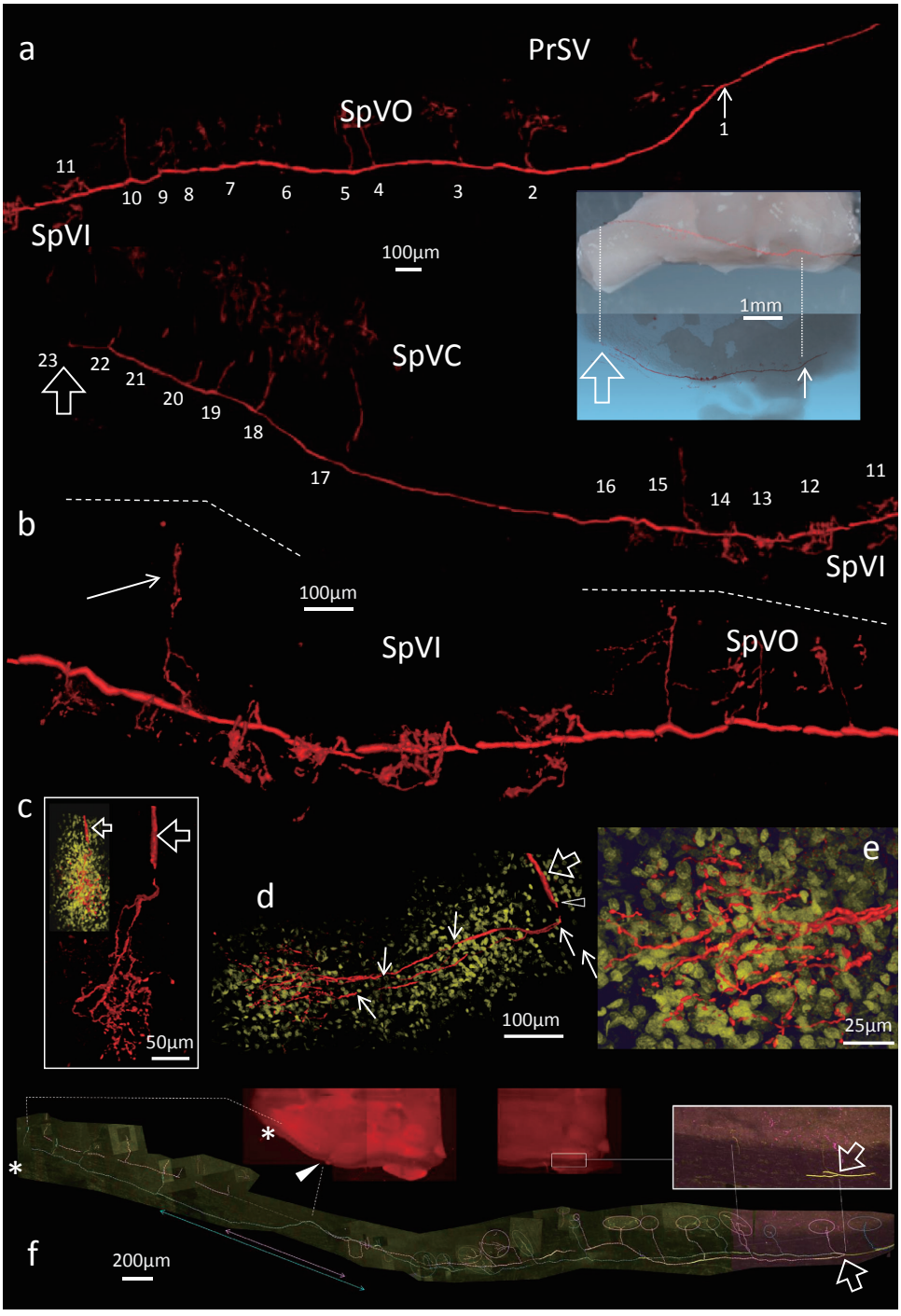

Fig. 5. (*Continued*) A collateral extended toward medial part of the nucleus (arrow). c) Montage of three-dimensional reconstructions produced from higher resolution confocal images of one of collaterals of labelled central branch (open arrow). In the upper left insertion, non-specific nuclei of cell bodies were visualized by DAPI (yellow) at the same time. d) A dorsal-ventral view of the c. The central branch (open arrow) produced one collateral (open arrowhead) prior to totally 4 divisions into two respectively. e) A higher magnification of the glomerular-like terminal arborization in d. f) An instance of a bifurcated central parent afferent in a labelled neuron with club-like ending. The bifurcated labelled afferents in addition to their collaterals were traced (in pink and yellow respectively) to the end of the central branches of the neuron (asterisk) through the level of obex (arrowhead on a horizontal section of the brainstem). Collaterals terminated respectively in the trigeminal nuclei (open circles). Labelled both parent afferents emitted no collaterals at a level across the obex (double-headed arrows).

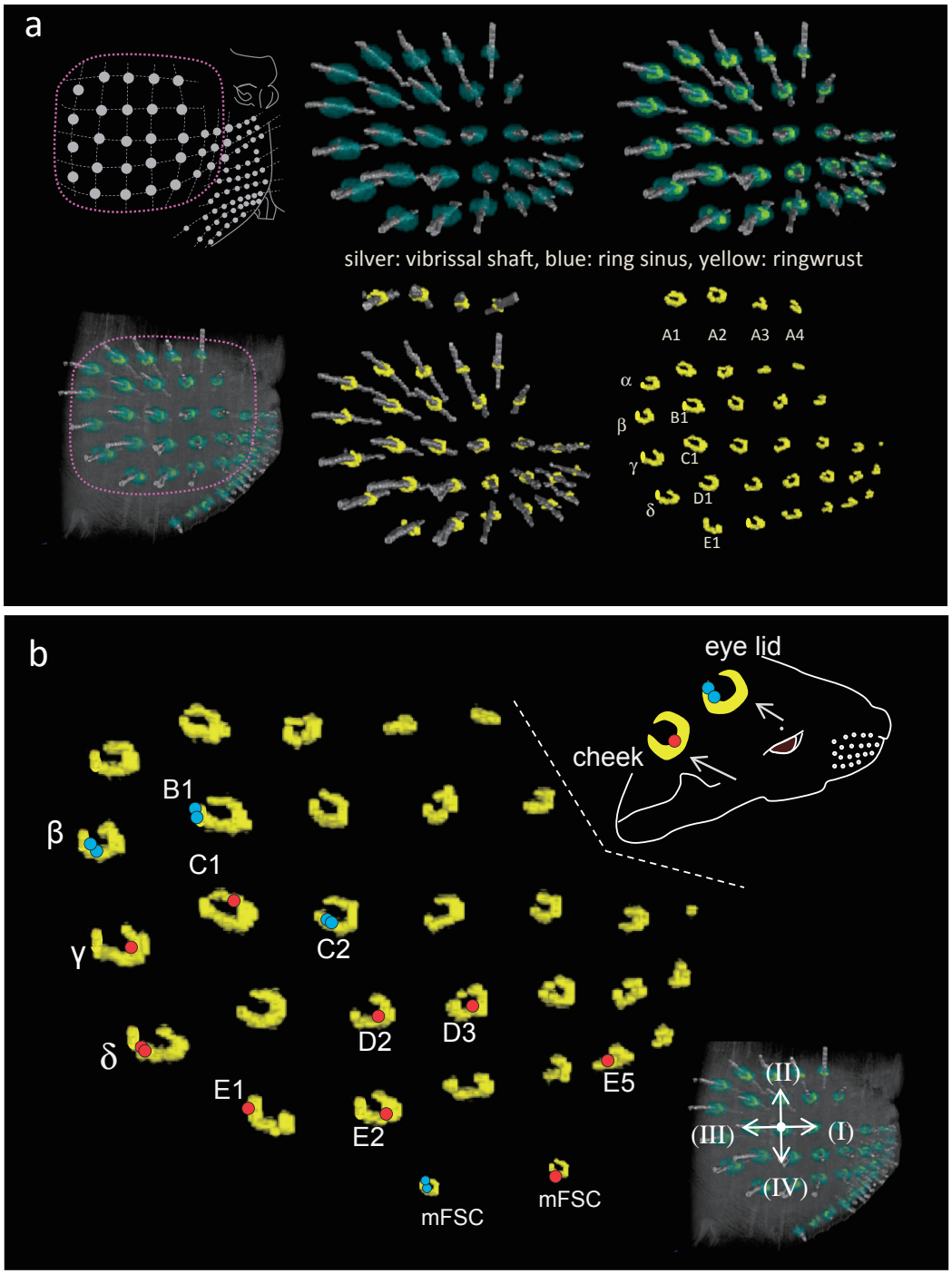

Fig. 6. a) At upper left, schematic drawings showing the arrangements of mystacial vibrissal follicles on the right snout. Next are 5 sets of reconstructed images showing the distributions of vibrissal follicles with sausage-like ringwulsts (yellow) surrounding each vibrissal shaft (silver) at the bottom level of the ring sinus (blue). These images were provided by tracing each structure in serial 1 µm thick plastic sections and all were reconstructed in three dimensions. Only 4 vibrissae of row A were presented in a different angle of view at the top of the figure. All ringwulsts display an open area dorso-caudally. b) Locations of each 16 club-like endings of labelled 16 TG neurons (β, γ, δ (2), B1, C1, C2, D2, D3, E1, E2, E5 and labial small FSCs (micro FSC (mFSC); 2), the rostral FSC on the eye lid, and the FSC on the cheek skin). Each dot indicates the position on the Rw of the ending. Five neurons (β, B1, C2 and caudal labial mFSC, and eye lid) showed bifurcated endings (blue dots). The other neurons terminated in only one club-like ending (red dot). Arrows on the lower right insertion indicate rostral (I), dorsal (II), caudal (III) and ventral (IV) directions respectively on the C2 whisker.

Central processes of labelled neurons with club-like endings. In contrast to the simple organization of peripheral processes of the club-like endings, central processes typically emitted approximately 20 collaterals that divided into multiple terminal branches in the trigeminal nuclei (Figs. 4b, 5). Some central processes (parent axons) extended to the level of the first cervical segment of the spinal cord (Figs. 4b, 5). Most parent axons were not bifurcated until the terminal region where the parent axon made a curve and terminated as the final collateral (Fig. 5). In this study the terminal curves were observed in 5 neurons with club-like endings, having a total of 18, 21, 21, 23 and 26 collaterals. The other parent axons that gradually faded from sight were considered to be unstained (See Ref. 19).

Most collaterals sprout from the parent axon at right angles (Fig. 5a), and are unbranched between their origins and their 'bush-like' terminal arborizations; however, several collaterals were observed to branch a few times before termination (Figs. 5c–e). Many parent axons contained lengths that were devoid or nearly devoid of collateral branches (Fig. 5), a phenomenon that was observed in all types of mechanoreceptor neurons, particularly in the region of the obex.

The central process of one neuron with a club-like ending branched into two daughter axons immediately after the emission of the second collateral (Fig. 5f). Those two daughter axons ran parallel to each other until their termination in the upper cervical segment of spinal cord, where a number of collaterals sprouted from them (26 in total). As observed in three-dimensional reconstruction, the terminal arborizations of these collaterals did not overlap. Another neuron in this study which also possessed a dividing morphology of the parent axons was identified as a neuron with a Merkel ending (data not shown).

Major differences of collateral sprouting of parent axons and of terminal arbors were indistinguishable among the various mechanoreceptor types examined 12 (club (5), Merkel (5), lanceolate (2) in FSCs) successfully labelled neurons in this study (data not shown).

Discussion

Intracellular approaches to analysis of trigeminal ganglion neurons. In this study, *in vivo* intracellular recordings and labelling permitted nearly the entire extent of single TG cells to be labelled and their responses to mechanical stimulation of the facial skin to be obtained. Results confirmed that primary sensory neurons are pseudo-unipolar cells,[1),20)] and for the first time, the visualization of the peripheral and central processes of single TG neurons, and their electrophysiological responses were achieved. Li *et al.*[21),22)] demonstrated similar aspects of pseudo-unipolar cells in the dorsal root ganglion neurons and in both newborn rats and mice in *ex vivo* preparations.

The central processes, that convey information by stages from brainstem to thalamus and eventually to the somatosensory cortex, have been investigated intensively using both morphological and physiological approaches.[9)–12),15)] In each relay station, the cell bodies are arranged in a matrix that topographically represents the peripheral arrangement of whiskers on the mystacial pad. Cell aggregates in each matrix are termed "barrelettes" (trigeminal nuclei), "barreloids" (thalamus) and "barrels" (somatosensory cortex); together,[7),8),13),14)] these regions comprise the whisker/barrel system.

The primary sensory neurons encode the first step of sensory input entering into the system. However, the way by which different mechanoreceptor types of primary neurons encode sensory inputs, that is, their electrophysiological responses, has yet to be determined. The present study is geared towards increasing our understanding of the processes involved in the encoding of information provided by mechanoreceptors. Subsequently, the studies of Li *et al.*[21),22)] demonstrated that axon terminals having various adaptation properties are combined in the arrays of longitudinal lanceolate endings, whereas in the present study, in both structure and function, the club-like endings were able to be characterized as a unique mechanoreceptor type.

Intra-axonal labelling constitutes a powerful methodology but it often fails to label both central and peripheral terminations mainly due to insufficient infiltration of the injected neuronal tracers.[9),10),19)] In recent years, studies have achieved successful intracellular labelling using *ex vivo* preparations of newborn rats and transgenic mice.[20)–22)] These studies demonstrated that single labelled dorsal root ganglion neurons that have particular mechanoreceptors in the skin of the back, and central processes and terminations in the dorsal horn of the spinal cord, respond to specific stimuli applied to their receptive fields, and represent a characteristic adaptation of the mechanoreceptor.

Using transgenic mice, these studies have revealed an exquisite organization of several kinds

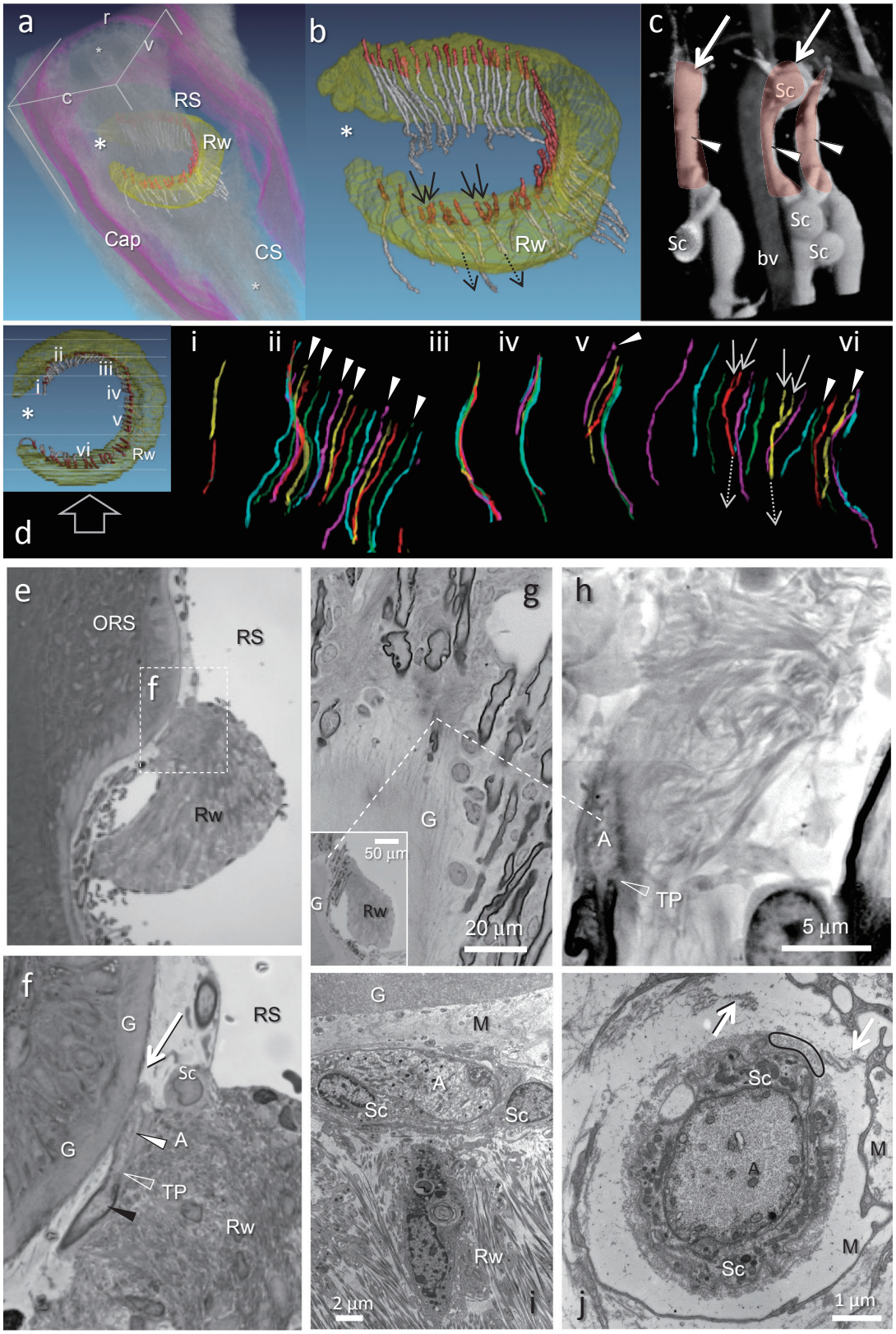
a
r
v
c
RS
Rw
Cap
CS
b
Rw
c
Sc
Sc
Sc
bv
Sc
d
i
ii
iii
iv
v
vi
Rw
e
ORS
RS
f
Rw
g
G
50 µm
G
Rw
20 µm
h
A
TP
5 µm
f
G
RS
Sc
A
G
TP
Rw
G
M
A
Sc
Sc
Rw
2 µm
i
Sc
M
A
M
Sc
1 µm
j

(Fig. 7)

of endings overlapping in the hairy skin of the back that correlate spatially with their terminations in the dorsal horn of the spinal cord. These investigators suggested a principal locus, mainly laminae II–III of the dorsal horn, for their integration and processing.[22] Investigations *in vivo* using intracellular analyses of trigeminal primary sensory neurons are likely to provide a degree of understanding comparable to that achieved in the *ex vivo* studies cited above.

Peripheral process organization. To date, both physiological analyses and morphological investigations separately have supported the hypothesis that each peripheral process of a primary sensory neuron has just one type of mechanoreceptor.[21),23),24)] The results of our morphological investigations using single fiber tracing demonstrate conclusively that the peripheral process of each TG neuron does indeed terminate as just one type of mechanoreceptor. In addition, we observed that intracellularly labelled peripheral processes display no ramifications along their course from the TG cell body up to their receptive fields.

No peripheral terminations of labelled neurons were detected in other areas of the facial skin. This finding may be related to recording and labelling within a limited area of the trigeminal ganglion, *i.e.*, an area situated in the lateral half and posterior regions of the TG close to the mandibular branch. Leiser and Moxon[25] report that trigeminal neurons recorded from the medial-half of the trigeminal ganglion have various receptive fields in the facial skin including all major mystacial vibrissae. More than 70% of the neurons innervating the mystacial vibrissae responded to stimulation of the upper A–C rows, whereas our results from 16 neurons with club-like endings primarily innervate vibrissae in the lower rows (C–E and small vibrissae). These results are consistent with the previously described topographic, dorso-ventral ordering of the facial vibrissae which correlates with the medio-lateral arrangement of ganglion cell bodies in the adult rat.[26),27)]

Club-like endings. The club-like ending is a unique and relatively simple sensory receptor distributed only within the FSC. Originally, the club-like ending was identified as the cut end of a nerve fiber or a kind of lanceolate endings[2),3)] until it was determined to be a true sensory terminal closely related to the ringwulst.[6)]

Tracing nerve fibers using neurobiotin, coupled with the reconstruction of serial semi-thin sections, demonstrated that most club-like endings exist solely at the tip of each myelinated axon. In addition, our findings suggest that mostly single, and rarely two club-like endings originate from individual TG neurons. Thus, the club-like ending basically displays a relatively simple morphology being the simplest structure observed so far among all types of mechanoreceptors.

Neurons having club-like endings elicit a much higher frequency of firing during air puff stimulation than the 3 other kinds of mechanoreceptors situated within the FSCs. In addition, only neurons with club-like endings have been observed to detect and

Fig. 7. a) A reconstruction of serial 1 µm plastic sections showing the position of the ringwulst rendered in yellow (Rw) within a follicle sinus complex (FSC) displayed in an oblique view from caudal (c) to rostral (r); ventral plane (v). Club-like endings shown in red, small asterisks indicate the vibrissal shaft. RS; ring sinus, Cap; capsule, CS; cavernous sinus. b) Higher magnification of the ringwulst (Rw) reconstructed from individual club-like endings (red) with their preterminal axons (white). All but 4 endings (arrows) were attached to a single axon. The exceptions converged as pairs of endings (solid arrows) into a single axon (dotted arrows). No club-like endings were observed at the open portion of the Rw (large asterisk. Also in a and d). c) Reconstruction of confocal images illustrating club-like endings; arrows point to spherical enlargements at their tips (see d, f). Schwann cells (Sc) envelope club-like endings (arrowheads). bv; blood vessel. d) Reconstruction of all 52 club-like endings in the ringwulst (Rw). Club-like endings were divided into 6 groups (i–vi) and colored as an aid to counting them. Typically, each club-like ending is associated with a single peripheral afferent, but in two instances, afferents bifurcated (solid white arrow; branch, dashed white arrow; parent fiber). Open arrow indicates view direction on the Rw for the colorful nerves. Nine of the 52 endings terminated in a ball-like appendage (arrowhead). e, f) A photomicrograph depicting within the ring sinus (RS), the ringwulst (Rw) attached to the outer root sheath (ORS). f) A High magnification of a square area in e. Black arrowhead; myelinated portion of a peripheral process, a filled white arrowhead; axon terminal of a peripheral process, TP; terminal point of myelination, G; glassy membrane, Sc; Schwann cell, RS; ring sinus, Rw; ringwulst, White arrow; a spherical enlargement at the tip of the club-like ending (see c). g, h) Observations of one of serial 1 µm-thick sections by a scanning electron microscope. Axon terminal (A) of club-like ending carried dense collagen fibrils connecting with the ringwulst (Rw) at a part of the opposite side to the glassy membrane (G). Dashed lines indicate the locations of these photographs at different magnifications. TP; terminal point of myelination. i) Electron micrograph depicting an axon terminal (A) adjacent to two Schwann cells (Sc), together these comprise a club-like ending. The Schwann cells are separated from the glassy membrane (G) by a mesenchymal sheath (M). j) Electron micrograph of a cross-sectioned axon terminal (A) enveloped by a Schwann cell (Sc) sheath, a layer of cross-sectioned collagen fibrils (*e.g.*, within black oval), and finally, a layer of mesenchyme (M), arrows; fine collagen bundles connected in places between inner capsular collagen fibrils and the thin cell layer.

respond to the most delicate mechanical movements evoked by air puff stimulation, whereas other kinds of mechanoreceptors are much less responsive. A detailed analysis of the electrophysiological properties of neurons having club-like endings will be provided in a subsequent paper (in preparation).

Neurophysiological studies have shown that trigeminal primary neurons are exquisitely sensitive to small whisker deflections.[28)–30)] Gottschaldt and Vahle-Hinz[31)] suggested that these cells can encode high frequency vibrations (up to 1.5 kHz) in a one-to-one manner, although they were estimated to have Merkel endings. Deschênes *et al.*[32)] indicated that primary vibrissal afferents are able to follow trains of sinusoidal deflections applied at frequencies up to 1 kHz in a phase-locked manner. Grady *et al.*[33)] demonstrated high-frequency whisker displacement during air puff stimulation at millisecond temporal resolution. Furthermore, we recorded a few neurons that fired at a frequency higher than 500 Hz during the same air puff stimulation (10 s, 0.1–0.03 MPa) of the mystacial pad in preliminary trials (data not shown). Our results suggest that a certain number of neurons, which were detected in extracellular recordings, and whose mechanoreceptor types were previously classified, could in fact be neurons with club-like endings, that fit the unique firing patterns observed here. Further quantitative investigations using various frequencies of mechanical stimulation would be necessary to classify mechanoreceptors precisely.

Ringwulst. The ringwulst has a unique shape and is situated within the ring sinus[34)] such that movements of the vibrissae are likely to produce corresponding movements of the ringwulst. A large portion of all club-like endings is situated between the glassy membrane and the ringwulst; the glassy membrane is separated from the club-like endings by a layer of mesenchyme, whereas the ringwulst is tightly connected by collagen fibers to the club-like endings.[2),35)–37)] (Figs. 7f, i). These morphological characteristics suggest that the club-like endings respond to the movement of the ringwulst. Alternatively, the ringwulst might more likely serve to buffer the club-like endings from movements other than those caused by the vibrissal shaft. This also suggests a significant difference between the functional mechanism of club-like endings and that of all other mechanoreceptors distributed close to the glassy membrane. For example, lanceolate endings are usually attached to the glassy membrane,[22),38)] and the axon terminals of Merkel endings at the level of the ring sinus are situated inside the glassy membrane, that is, in the outer root sheath.[6)]

Rice *et al.*[2)] regarded the ringwulst as a balancing toy floating within the ring sinus. The cause of the movement is still unknown but it may be that blood pressure within the ring sinus would produce a delay of the movement of the ringwulst from the initial movement of the vibrissal follicle. In addition, the ringwulst may be moved in one piece within the blood sinus in contrast to the other part of the ringwulst, (*i.e.*, the outer root sheath and mesenchymal sheath of the follicle), which is able to be moved only in a restricted direction under the direct effect of the movement of the vibrissal shaft. Moreover, the ringwulst has an "opening" in its side oriented in a dorso-medial direction; there are few club-like endings within the opening.

Using single axonal recordings and tracing methods, Furuta *et al.* (in preparation) demonstrated in rat that some of the mechanoreceptors in the FSCs display a particular orientation selectivity for vibrissal movement. Club-like endings, because of their palisade-like arrangement associated with the unique structure of the ringwulst, may play a specific role in receiving essential information for discriminating the orientation of movement of the vibrissal shaft.

Our results suggest strongly that the ringwulst has some very specific mechanisms involving a more dense innervation than other regions of the FSC. Our results also suggest that neurons having club-like endings can respond adaptably to delicate vibrations of the hair shaft, evoking high-frequency action potentials. In contrast to the club-like endings, reticular endings, display a voluminous branching within their receptive fields (Fig. 2, and *cf.*)[6)] and can respond to a long-lasting deformation of the follicle at the cavernous sinus, evoking continuous firing. In addition to the characteristic responses with relatively simple morphology of neurons with club-like endings, we estimate that more than 40 TG neurons surround and innervate a limited belt zone at the neck of the floating ringwulst. Club-like endings associated with the ringwulst within the ring sinus present an ideal model to investigate a mechanism of mechanoreception. Questions such as how movements of the ringwulst are related to whisker stimulation, or whether all the endings respond at the same time or not, and the character of their central neurotransmission *etc.*, are expected to be the subject of future investigations that include computer simulation studies.

Number of neurons innervating the ringwulst. The variability of the labelled 51 mechanoreceptor neurons in this study (Table 1) is insufficient for determining their accurate distribution in the facial skin, as many samples whose receptive fields did not include any FSCs were excluded from this study. In contrast, our data on 40 mechanoreceptors detected in the FSCs provide a reliable estimate of the distribution of mechanoreceptors within the FSC.

Five axons of 16 labelled club-like endings bifurcated for the first time within the FSC. Only one of them displayed a side-by-side termination. The remaining 4 bifurcated at the lower level of the FSC, their individual branches terminated as solitary club-like endings.

Four of 52 club-like endings traced in the three-dimensional reconstruction of serial 1 µm-thick sections were also of the side-by-side type. In this reconstruction, bifurcated but not side-by-side types might not be represented even if they existed, because all myelinated axons were traced only within a restricted region in which the ringwulst was observed simultaneously, thus limiting our field of view. When calculating the probability of bifurcation to be 5/16 and side-by-side probability to be 1/5, then in a FSC in which 52 club-like endings occur, we estimate that 16 club-like endings would be bifurcated and 3 would be in the side-by-side category. The fact that a very similar number of afferents (4 side-by-side of the 52 club-like endings) were depicted in the reconstruction of 1 µm-thick sections, indicates the validity of our findings. Further, the estimated number of neurons innervating a single FSC, in which 52 club-like endings where counted, is 44 (assuming that 16 club-like endings bifurcated).

According to a previous estimation that about 150 myelinated afferents in a deep vibrissal nerve should innervate individual FSCs,[2] more than 30% of them should terminate as club-like endings, that innervate only the ringwulst. Our results do not show the exact number of neurons innervating single FSCs, however, we were able to determine that 40% of all labelled neurons in this study that innervated FSCs were in fact club-like endings. Further quantitative investigations on a larger number of FSCs would greatly assist in the refining of our current estimates.

Central process organization. Previous studies have investigated whether the response properties of primary sensory neurons are predictors of the morphology of the terminal distributions within the trigeminal nuclei.[9),10),16),19)] Hayashi clearly presented whole horizontal views of branching collaterals at regular intervals from intra-axonally labelled stem axons innervating FSCs throughout the trigeminal tract and nuclei.[39)] He also mentioned that one stem axon divided into two daughter axons inside the tract at the level of trigeminal subnucleus interpolaris and that those collaterals did not overlap.[19)] Results of his and Jacquin's groups stated that trigeminal primary afferents associated with mystacial vibrissae are not predictors of differences in central morphology.[10),19),39)]

Our observations of the 12 labelled neurons are consistent with those previous findings, and in addition, individual mechanoreceptors in their receptive fields were all identified and characterized in this study. Regardless of the small number of successfully-reconstructed neurons of each mechanoreceptor type, and a less precise morphological analysis of collateral branching patterns, our three-dimensional reconstructions suggest that no major differences exist between the central processes of mechanoreceptors of different types. Further analysis is required to verify this conclusion.

We recognized some parent afferents with a portion of rare sprouting collaterals around the level of obex. This accords with the study of Hayashi,[39)] who showed that the density of collaterals was maintained at about 1.2 collaterals per 0.5 mm of stem axon at the level of the trigeminal subnucleus interpolaris, but decreased abruptly just caudal to the obex. Regarding the locations of collateral branches emitted by the central primary afferents observed in this study, our findings confirm those of Hayashi. Because the absence of collaterals was observed for all types of mechanoreceptors, it is possible that this feature is a general characteristic of mechanoreceptors.

Matching properties between primary sensory neurons and their post-synaptic targets might be demonstrated at a later stage, but at present, the data do not support this thesis. The density of the collaterals of central processes may be the major factor in determining the tactile stimulation that is encoded even by the simplest mechanoreceptor, the club-like ending.

In conclusion the results of this study constitute a breakthrough in the analysis of the organization and properties of vibrissa related mechanoreceptors. Our findings lay the basis for future attempts to decode the information obtained by mechanoreceptors and their associated TG neurons situated at the very beginning of the vibrissae-barrel neuraxis.

Acknowledgements

We are grateful to Drs. Keiji Imoto (National Institute of Physiological Science, Japan), Takeshi Kaneko (Kyoto University, Japan), Megumu Yoshimura (Kumamoto Health Science University, Japan) and John Heuser (Kyoto University, Japan) for invaluable supports for our projects. We also express appreciation to Drs. Sachi Ohno (Kagoshima University, Japan), Daichi Hirai (Kyoto University, Japan), Junichi Hachisuka (Kyushu University, Japan) and Toshiyuki Saji (National Institute of Science, Japan) for their excellent technical help in support of our preliminary and present studies. We appreciate the efforts of Dr. Edward L. White (Ben Gurion University, Israel) for his editing of the manuscript, and those of Dr. Dana Sherman (Weizmann Institute of Science, Israel) for her careful reading of the manuscript.

References

1) Retzius, G. (1880) Untersuchungen uber die- Norvensellen der cerebrospinalen. Ganglien und der ubrigen periferschen. Kopfganglien mit besonderer. Berucksichtigung auf die zellenaus laufer. *In* Arch. Anat. Physiol., Antomiche Abtheilung (eds. His, W., Braune, W. and Bois-Reymond, E.D.). Verlag von Veit & Comp., Leipzig, pp. 369–402.
2) Rice, F.L. and Munger, B.L. (1986) A comparative light microscopic analysis of the sensory innervation of the mystacial pad. I. Innervation of vibrissal follicle-sinus complexes. J. Comp. Neurol. **252**, 186–205.
3) Rice, F.L., Kinnman, E., Aldskogius, H., Johansson, O. and Arvidsson, J. (1993) The innervation of the mystacial pad of the rat as revealed by PGP 9.5 immunofluorescence. J. Comp. Neurol. **337**, 366–385.
4) Fundin, B.T., Arvidsson, J. and Rice, F.L. (1995) Innervation of nonmystacial vibrissae in the adult rat. J. Comp. Neurol. **357**, 501–512.
5) Rice, F.L., Fundin, B.T., Arvidsson, J., Aldskogius, H. and Johansson, O. (1997) Comprehensive immunofluorescence and lectin binding analysis of vibrissal follicle sinus complex innervation in the mystacial pad of the rat. J. Comp. Neurol. **385**, 149–184.
6) Ebara, S., Kumamoto, K., Matsuura, T., Mazurkiewicz, J.E. and Rice, F.L. (2002) Similarities and differences in the innervation of mystacial vibrissal follicle-sinus complexes in the rat and cat: a confocal microscopic study. J. Comp. Neurol. **449**, 103–119.
7) Woolsey, T.A. and Van der Loos, H. (1970) The structural organization of layer IV in the somatosensory region (SI) of mouse cerebral cortex. The description of a cortical field composed of discrete cytoarchitectonic units. Brain Res. **17**, 205–242.
8) Van der Loos, H. and Woolsey, T.A. (1973) Somatosensory cortex: structural alterations following early injury to sense organs. Science **179**, 395–398.
9) Jacquin, M.F., Woerner, D., Szczepanik, A.M., Riecker, V., Mooney, R.D. and Rhoades, R.W. (1986) Structure-function relationships in rat brainstem subnucleus interpolaris. I. Vibrissa primary afferents. J. Comp. Neurol. **243**, 266–279.
10) Jacquin, M.F., Renehan, W.E., Mooney, R.D. and Rhoades, R.W. (1986) Structure-function relationships in rat medullary and cervical dorsal horns. I. Trigeminal primary afferents. J. Neurophysiol. **55**, 1153–1186.
11) Capra, N.F. and Dessem, D. (1992) Central connections of trigeminal primary afferent neurons: topographical and functional considerations. Crit. Rev. Oral Biol. Med. **4**, 1–52.
12) Jacquin, M.F., Renehan, W.E., Rhoades, R.W. and Panneton, W.M. (1993) Morphology and topography of identified primary afferents in trigeminal subnuclei principalis and oralis. J. Neurophysiol. **70**, 1911–1936.
13) Waite, P.M.E. and Tracey, D.J. (1995) Trigeminal sensory system. *In* The rat nervous system, Second edition (ed. Paxinos, G.). Academic Press, New York, pp. 705–724.
14) Haidarliu, S. and Ahissar, E. (2001) Size gradients of barreloids in the rat thalamus. J. Comp. Neurol. **429**, 372–387.
15) Bosman, L.W., Houweling, A.R., Owens, C.B., Tanke, N., Shevchouk, O.T., Rahmati, N., Teunissen, W.H., Ju, C., Gong, W., Koekkoek, S.K. and De Zeeuw, C.I. (2011) Anatomical pathways involved in generating and sensing rhythmic whisker movements. Front. Integr. Neurosci. **5**, 53.
16) Tonomura, S., Ebara, S., Uta, D., Furue, H., Furuta, T., Kuroda, D. and Kumamoto, K. (2015) Three dimensional reconstruction of trigeminal ganglion cell processes labelled by intracellular injection; Emphasis on club-like endings. J. Phisyol. Sci. **65**, S275.
17) Furuta, T., Kaneko, T. and Deschênes, M. (2009) Septal neurons in barrel cortex derive their receptive field input from the lemniscal pathway. J. Neurosci. **29**, 4089–4095.
18) Ebara, S., Kumamoto, K., Baumann, K.I. and Halata, Z. (2008) Three-dimensional analyses of touch domes in the hairy skin of the cat paw reveal morphological substrates for complex sensory processing. Neurosci. Res. **61**, 159–171.
19) Hayashi, H. (1985) Morphology of central terminations of intra-axonally stained, large, myelinated primary afferent fibers from facial skin in the rat. J. Comp. Neurol. **237**, 195–215.
20) Woodbury, C.J. and Koerber, H.R. (2007) Central and peripheral anatomy of slowly adapting type I low-threshold mechanoreceptors innervating parent skin of neonatal mice. J. Comp. Neurol. **505**, 547–561.
21) Li, L., Rutlin, M., Abraira, V.E., Cassidy, C., Kus,

L., Gong, S., Jankowski, M.P., Luo, W., Heintz, N., Koerber, H.R., Woodbury, C.J. and Ginty, D.D. (2011) The functional organization of cutaneous low-threshold mechanosensory neurons. Cell **147**, 1615–1627.
22) Li, L. and Ginty, D.D. (2014) The structure and organization of lanceolate mechanosensory complexes at mouse hair follicles. Elife **3**, e01901.
23) Bennett, D.L., Michael, G.J., Ramachandran, N., Munson, J.B., Averill, S., Averill, S., Yan, Q., McMahon, S.B. and Priestley, J.V. (1998) A Distinct Subgroup of Small DRG Cells Express GDNF Receptor Components and GDNF Is Protective for These Neurons after Nerve Injury. J. Neurosci. **18**, 3059–3072.
24) Suzuki, M., Ebara, S., Koike, T., Tonomura, S. and Kumamoto, K. (2012) How many hair follicles are innervated by one afferent axon? A confocal microscopic analysis of palisade endings in the auricular skin of thy1-YFP transgenic mouse. Proc. Jpn. Acad., Ser. B, Phys. Biol. Sci. **88**, 583–595.
25) Leiser, S.C. and Moxon, K.A. (2006) Relationship between physiological response type (RA and SA) and vibrissal receptive field of neurons within the rat trigeminal ganglion. J. Neurophysiol. **95**, 3129–3145.
26) Rhoades, R.W., Chiaia, N.L. and Macdonald, G.J. (1990) Topographic organization of the peripheral projections of the trigeminal ganglion in the fetal rat. Somatosens. Mot. Res. **7**, 67–84.
27) Erzurumlu, S.R., Murakami, Y. and Rijli, F.M. (2010) Mapping the face in the somatosensory brainstem. Nat. Rev. Neurosci. **11**, 252–263.
28) Zucker, E. and Welker, W.I. (1969) Coding of somatic sensory input by vibrissae neurons in the rat's trigeminal ganglion. Brain Res. **12**, 138–156.
29) Gibson, J.M. and Welker, W.I. (1983) Quantitative studies of stimulus coding in first-order vibrissa afferents of rats. 1. Receptive field properties and threshold distributions. Somatosens. Mot. Res. **1**, 51–67.
30) Shoykhet, M., Doherty, D. and Simons, D.J. (2000) Coding of deflection velocity and amplitude by whisker primary afferent neurons: implications for higher level processing. Somatosens. Mot. Res. **17**, 171–180.
31) Gottschaldt, K.M. and Vahle-Hinz, C. (1981) Merkel cell receptors: structure and transducer function. Science **214**, 183–186.
32) Deschênes, M., Timofeeva, E. and Lavallée, P. (2003) The Relay of High-Frequency Sensory Signals in the Whisker-to-barreloid pathway. J. Neurosci. **23**, 6778–6787.
33) Grady, S.K., Hoang, T.T., Gautam, S.H. and Shew, W.L. (2013) Millisecond, micron precision multi-whisker detector. PLoS One **8**, e73357.
34) Vincent, S.B. (1913) The tactile hair of the white rat. J. Comp. Neurol. **23**, 1–34. Berlin, New York, pp. 3–28.
35) Patrizi, G. and Munger, B.L. (1966) The ultrastructure and innervation of rat vibrissae. J. Comp. Neurol. **126**, 423–435.
36) Munger, B.L. and Rice, F.L. (1986) Successive waves of differentiation of cutaneous afferents in rat mystacial skin. J. Comp. Neurol. **252**, 404–414.
37) Halata, Z. (1993) Sensory innervation of the hairy skin (light- and electron microscopic study). J. Invest. Dermatol. **101**, 75S–81S.
38) Takahashi-Iwanaga, H. (2000) Three-dimensional microanatomy of longitudinal lanceolate endings in rat vibrissae. J. Comp. Neurol. **426**, 259–269.
39) Hayashi, H. (1980) Distributions of vibrissae afferent fiber collaterals in the trigeminal nuclei as revealed by intra-axonal injection of horseradish peroxidise. Brain Res. **183**, 442–446.

(Received Sep. 29, 2015; accepted Oct. 29, 2015)